Vol. 43 (2000), 2, 302-310
TRIBOLOGY TRANSACTIONS

The Dynamic Properties of Annular Gas Squeeze Film Dampers©

BRAD A. MILLER and ITZHAK GREEN
Georgia Institute of Technology
George W. Woodruff School of Mechanical Engineering
Atlanta, Georgia 30332-0405

The step jump method is used to characterize the stiffness and damping of flat-faced gas lubricated squeeze film dampers. Analytic solution of a linearized form of the isothermal and compressible Reynolds equation yields closed form expressions for the step and frequency responses of the gas film. Results from the step jump method obtained both analytically and numerically are shown to be good approximations of the gas film stiffness and damping. A Prony series is proven to be an effective constitutive model capable of representing the stiffness and damping of the gas film in both the time and frequency domains in analytic form. Using the analytic constitutive model, closed form solutions for the motion of squeeze film dampers are now possible.

Presented at the 54th Annual Meeting
Las Vegas, Nevada
May 23-27, 1999
Final Manuscript approved July 14, 1999

KEY WORDS

Squeeze-Film Lubrication; Fourier Transform Infrared Spectroscopy; Dampers

INTRODUCTION

The gas film has a significant effect on the motion of squeeze film dampers. It stores and dissipates energy, and these properties are time transient and frequency dependent. Ideally, the designer would like to know the stiffness and damping provided by the gas film at an early stage in the design process. This would allow optimization of the operating characteristics for the specific application, whether it is maximizing stiffness and damping or predicting stability of the overall mechanism. Therefore, it is important to quantify the contribution from the gas film. Also, the method of determining these characteristics should be time efficient and accurate.

NOMENCLATURE

A	= surface area of Annuli A and B
A_n, B_n, C_n, D_n, d_n	= constant coefficients
$b_{er}, b_{ei}, k_{er}, k_{ei}$	= Kelvin functions
$d_{sz}, d_{s\gamma}$	= support damping constants in axial and angular modes, respectively
E_{ni}	= constant coefficient
δF_z^*	= net gas film force in z direction on Annulus A
δF_z	= nondimensional net gas film force in z direction on Annulus A, $\delta F_z^*/(P_a^* \cdot r_o^{*2})$
$\delta F_z(j\sigma)$	= Fourier transform of δF_z
$G^*(j\omega)$	= gas film frequency response
$G(j\sigma)$	= nondimensional gas film frequency response, $G^*(j\omega) \cdot h_o^*/(P_a^* \cdot r_o^{*2})$
$G'(j\sigma)$	= real part of $G(j\sigma)$, storage modulus
$G''(j\sigma)$	= imaginary part of $G(j\sigma)$, loss modulus
h^*	= gas film thickness
h_o^*	= clearance between centers of Annulus A and Annulus B at equilibrium
h	= nondimensional gas film thickness, h^*/h_o^*
Δh^*	= displacement amplitude
Δh	= nondimensional displacement amplitude, $\Delta h^*/h_o^*$
δh^*	= perturbation film thickness
δh	= nondimensional perturbation film thickness, $\delta h^*/h_o^*$
$\delta H(j\sigma)$	= Fourier transform of δh
I^*	= transverse moment of inertia of Annulus A about any diameter
I	= nondimensional moment of inertia of Annulus A, $I^* \cdot P_a \cdot h_o^{*5}/(144\ \mu^2 \cdot r_o^{*8})$
j	= imaginary unit, $(-1)^{1/2}$
J_n	= Bessel function of the first kind of order n
k_{fz}^*	= axial force step response
$k_{m\gamma}^*$	= moment step response
k_{fz}	= nondimensional axial force step response, $k^*(t) \cdot h_0^*/(P_a^* \cdot r_0^{*2})$
$k_{m\gamma}$	= nondimensional moment step response, $k^*(t) \cdot h_0^*/(P_a^* r_o^{*4})$
$K(s)$	= Laplace transform of k(t)
$K(j\sigma)$	= Fourier transform of k(t)
$k(\infty)$	= long time asymptotic value of k(t)
$k_{gz}, k_{g\gamma}$	= pseudo spring moduli
$k_{sz}, k_{s\gamma}$	= support spring moduli
m	= mass of Annulus A

m = nondimensional mass of Annulus A, $m^* \bullet P_a \bullet h_o^{*5} / (144\ \mu^2 \bullet r_o^{*6})$
δM_x^* = net gas film moment about x axis on Annulus A
δM_x = nondimensional net gas film moment about x axis on Annulus A, $\delta M_x^* / P_a \bullet r_o^{*3}$)
p^* = pressure
p = nondimensional pressure, p^*/P_a
P_a = ambient pressure
δp^* = perturbation pressure
δp = nondimensional perturbation pressure, $\delta p^*/P_a$
Q_n = constant coefficient
r^* = radial coordinate
r = nondimensional radial coordinate, r^*/r_o^*
r_i^* = inner radius
r_o^* = outer radius
r_s = radius location for support spring and damper
R_i = radius ratio, r_i^*/r_o^*
s = Laplace variable
t^* = time
t = nondimensional time, $\omega \bullet t^*$
Y_n = Bessel function of the second kind of order n
z^* = axial coordinate
z = nondimensional axial coordinate, z^*/h_o^*
$Z(s)$ = Laplace transform of z(t)
Δz^* = step jump magnitude in axial direction
Δz = nondimensional step jump magnitude, $\Delta z^*/h_o^*$
$Z(s)$ = Laplace transform of z(t)
$z^*(0)$ = initial position of Annulus A
$\dot{z}^*(0)$ = initial velocity of Annulus A
$\dot{z}(0)$ = initial nondimensional velocity of Annulus A, $\dot{z}^*(0) \bullet (12 \bullet \mu \bullet r_o^{*2})/(P_a \bullet h_o^{*3})$
α_n = decay parameter
γ^* = tilt coordinate
γ = nondimensional tilt coordinate, $\gamma^* \bullet r_o^*/h_o^*$
$\Gamma(s)$ = Laplace transform of $\gamma(t)$
$\Delta\gamma^*$ = step jump in tilt coordinate
$\Delta\gamma$ = nondimensional magnitude of step jump in tilt coordinate, $\Delta\gamma^* \bullet r_o^*/h_o^*$
λ = root of characteristic equation, decay parameter
μ = gas viscosity
σ = squeeze number, $12 \bullet \mu \bullet r_o^{*2} \bullet \omega/(P_a \bullet h_o^{*2})$
τ = modified nondimensional time parameter, t/σ
ω = excitation frequency

The gas film dynamic properties are found by solving the isothermal and compressible form of the Reynolds equation. This process is non-trivial since the Reynolds equation is nonlinear in pressure. For practical applications, no analytic solution is available for the flill nonlinear form of the Reynolds equation. Recently, however, Miller and Green (1998) have introduced an analytic technique for incorporating the gas film properties into the dynamic analysis of gas lubricated triboelements. Ihis technique is called the gas film correspondence principle, and it will be used here to analyze the dynamics of squeeze film dampers.

The gas film correspondence principle requires that the gas film be modeled by a constitutive model. This constitutive model represents analytically the stiffliess and damping of the gas film for all time and frequencies. The important consequence of this technique is that the constitutive model must only be calculated once foy a given set of gas film parameters. Once it is available, it completely characterizes the dynamic properties of the gas film. Then, using the gas film correspondence principle, the constitutive model is integrated into the equations of motion, and the analysis continues analytically, yielding closed form expressions for motion, transfer functions, and stability.

Choosing a thermodynamically valid analytic function to represent the constitutive model is important. Elrod et al. (1967) use a series of Laguerre Polynomials to model the gas film properties in a journal bearing, but Miller and Green (1997) prove that the model can violate the Second Law of Thermodynamics. Later, Miller and Green (1998) show that a Prony series is a flexible, thermodynamically valid gas film model useful for a wide range of applications. For this reason, a Prony series is used for the constitutive model in this work.

The gas film correspondence principle relies on the premise that the gas film forces and moments are linear with respect to the displacements. If this linearity assumption is valid, then the gas film properties can be represented by the step response (Elrod et al., 1967) or by the frequency response (Ono, 1975, and Blech, 1985).

The step response characterizes the gas film properties in the time domain. For the annular squeeze film damper, the step response can be calculated analytically by solution of the linear form of the Reynolds equation. For applications where the step response cannot be found analytically, a direct numerical technique introduced by Elrod et al. (1967) can be used. The frequency response characterizes the gas film properties in the frequency domain. Blech (1985) gives an analytic solution for the frequency response for annular squeeze film dampers. For applications where analytic solutions for the frequency response are not possible, the perturbation technique suggested by Ono (1975) can be used. The numerical technique introduced by Miller and Green (1998) for rectangular slider bearings can also be adapted to squeeze film dampers. Furthermore, any of the step responses calculated by the techniques discussed earlier can be transformed into the frequency domain to give the frequency response and vice versa. Once the step response or frequency response is calculated, the coefficients for the constitutive model are carefully chosen by a curve fit procedure.

For most practical tribological applications, the linearity assumption implied by the gas film correspondence principle and the step jump method is valid if motion is relatively small about the equilibrium state. Previous attempts to validate this assumption have relied solely on numerical solutions for the frequency response and step response (Miller and Green, 1997 and 1998). In this work, however, a squeeze film damper is considered for which analytic solutions for the frequency response and the step response are obtained. Just for comparison, the frequency response and step response are calculated numerically as well, and constitutive models for the gas film are derived from the four solutions. Then, closed form expressions for the motion are found with these four models using the gas film correspondence principle; these expressions are then compared to results from a direct numerical simulation. In all four cases, the results from the correspondence principle compare well with the direct numerical simulation.

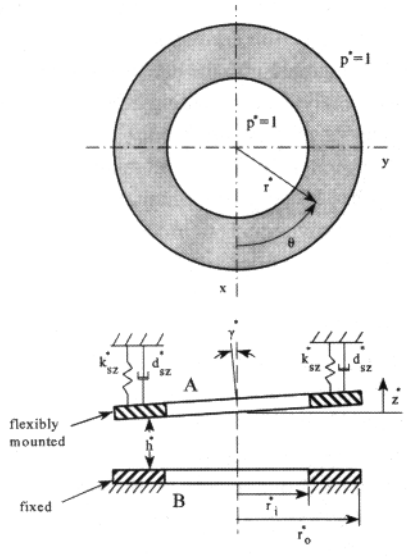

Fig. 1—Schematic of annular squeeze film damper.

TABLE 1—SQUEEZE FILM DAMPER PARAMETERS	
Ambient Pressure, P_a	0.1 MPa
Viscosity (air), μ	1.8 $(10)^{-5}$ Ns/m
Outer Radius, r_o^*	0.04 m
Clearance, h_o^*	2.0 μm
Axial support stiffness, k_{sz}	5.0 $(10)^7$ N/m
Axial support damping, d_{sz}	300 Ns/m
Angular support stiffness, $k_{s\gamma}$	4.0 $(10)^4$ Nm/rad
Angular support damping, $d_{s\gamma}$	0.24 Nm s/rad
Initial vertical velocity, $\dot{z}$ (0)	0.002 m/s
Initial angular velocity, $\dot{\gamma}$ (0)	0.05 rad/s

ANALYSIS

A schematic of a squeeze film damper is shown in Fig. 1. The springs and dampers indicated in the figure yield a total axial stiffness and damping for the support of k_{sz}^* and d_{sz}^*, respectively. These also give angular stiffness and damping about any tilt axis according to the following relationship (Green and Etsion, 1985),

$$k_{s\gamma}^* = \frac{1}{2} k_{sz}^* \cdot r_s^{*2}$$
$$d_{s\gamma}^* = \frac{1}{2} d_{sz}^* \cdot r_s^{*2} \qquad [1]$$

Here, the springs and dampers are assumed to be located at $r_s^* = r_o^*$ and to have uniform circumferential properties. Values for the geometry and other parameters are given in Table 1. A very thin film of air (relative to the physical geometry) separates the two rigid faces. Pressure is generated in this gap as a squeeze effect when the film thickness oscillates with respect to time. Annulus A is allowed to translate in the z direction and to tilt about a diameter. This tilt axis is essentially arbitrary since the gas film properties and support properties are the same for tilt about any axis.

The equation governing the pressure in the gas region is the isothermal and compressible form of the Reynolds equation. The nondimensional form of this equation is shown below in a polar coordinate reference frame (see the nomenclature for the nondimensional parameters).

$$\frac{\partial}{\partial r}\left(rph^3 \frac{\partial p}{\partial r} \right) + \frac{1}{r}\frac{\partial}{\partial \theta}\left(ph^3 \frac{\partial p}{\partial \theta} \right) = \sigma r \frac{\partial (ph)}{\partial t} \qquad [2]$$

The parameter, σ, is the squeeze number, and it is defined in the nomenclature. On the boundaries at r=R, and r=1, the pressure is ambient.

For the case of axial motion only (i.e., no tilt), the analysis presented here is valid regardless of whether Annulus B is fixed or rotating. Therefore, the results for axial motion are applicable to a flat-faced mechanical seal with no pressure difference across the seal.

To derive the linear form of Reynolds equation, consider the state when the motion is small and very close to the equilibrium height, such that h=1+δh. Likewise, the corresponding pressure generated, δp, is also assumed to be small in comparison to the ambient pressure, so that the total pressure is p =1 + δp. With these assumptions, the Reynolds equation can be linearized by small perturbation theory, yielding,

$$\frac{\partial}{\partial r}\left(r\frac{\partial \delta p}{\partial r} \right) + \frac{1}{r}\frac{\partial^2 \delta p}{\partial \theta^2} = \sigma r \left(\frac{\partial \delta p}{\partial t} + \frac{\partial \delta h}{\partial t} \right) \qquad [3]$$

Now, with the resulting equation in linear form, it is possible to find an exact solution for the step response as well as the frequency response.

STEP RESPONSE

For the geometry in Fig. 1, positive translation of Annulus A in the z direction results in an increase in the film thickness, δh. The step response is defined as the change in force or moment from their equilibrium values produced in response to a step jump in magnitude divided by the amplitude of the step jump. For the general case when the axial and angular modes are coupled, there will be four step responses: the force and moment responses to an axial displacement and the corresponding force and moment responses to a tilt displacement. However, for this application, the axial force response resulting from the tilt motion is negligible, and the moment response resulting from the axial motion is identically zero. Consequently, only the two direct responses are calculated.

The step jump occurs instantaneously at t=0 and is assumed to be an isothermal process, which is an assumption already postulated by the Reynolds equation. Mathematically, the step jump in axial displacement is δh = Δz u(t), where u(t) is a unit step function and Δz is the amplitude of the step jump. The step jump in tilt displacement is δh = Δγ rcos(θ)u(t). Once the initial step jump in displacement or tilt has occurred, the height does not change for t > 0, and Eq. [3] reduces to

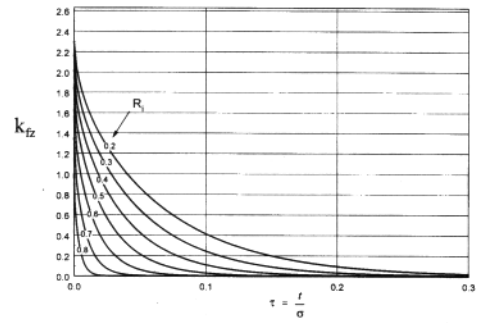

(a)

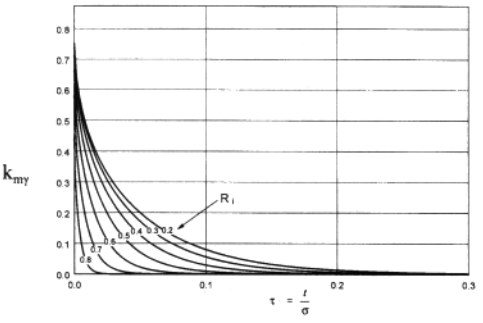

(b)

Fig. 2—(a) Analytical solution for force response to a step jump in axial displacement.
(b) Analytical solution for moment response to a step jump in tile about x axis.

$$\frac{\partial}{\partial r}\left(r\frac{\partial \delta p}{\partial r}\right)+\frac{1}{r}\frac{\partial^2 \delta p}{\partial \theta^2}=\sigma r\frac{\partial \delta p}{\partial t} \qquad [4]$$

subject to the following boundary conditions:

$$\delta p\ (R_i,\ t) = 0$$

$$\delta p\ (1,t)\ = 0$$

Etsion (1980) further simplifies Eq. [4] for radius ratios, R_i, that are close to unity using the narrow seal approximation. While this simplification may be justified for mechanical seals, this option may not be available for squeeze film dampers. Therefore, this simplification is not used here, and the following analysis is valid for any radius ratio.

Equation [4] is well known in the field of heat conduction. Following a method given by Powers (1987), the general solution for this type of equation for t > 0 is in the form below.

$$\delta p(r,t) = R(r)\cos(\theta)^n e^{-\frac{\lambda_i^2}{\sigma}t} \qquad [5]$$

In Eq. [5] and following, n=0 corresponds to axial motion, and n=1 corresponds to tilt motion. The decay parameter, λ_i, is the i^{th} root of the characteristic equation below.

$$J_n(\lambda R_i)\ Y_n\ (\lambda) - J_n\ (\lambda)\ Y_n\ (\lambda R_i) = 0 \qquad [6]$$

J_n is the Bessel function of the first kind of order n, and Y_n is the Bessel function of the second kind of order n.

The initial condition for the pressure comes from the physical process of the step jump itself. Since the Reynolds equation, Eq. [2], already assumes the gas to be isothermal, it is natural to assume that the step jump is also an isothermal process. Therefore, the equation of state for an ideal gas reduces to

$$\frac{p\cdot(h\cdot A)}{mass} = \text{constant} \quad @t=0 \qquad [7]$$

where A is the exposed annular area and (h•A) is the total volume of air between the annuli. The area, A, is constant, and the mass is also assumed to remain constant through the instantaneous step process, so the following initial conditions are imposed on the pressure inside the annular region, excluding the boundaries.

$$\delta p = -\Delta z \qquad @\ t=0^+ \quad \text{axial motion}$$

$$\delta p = -r\Delta\gamma\cos(\theta) \quad @\ t=0^+ \quad \text{tilt motion} \qquad [8]$$

The complete solution for Eq. [4] that satisfies the boundary conditions is an infinite series of Bessel functions,

$$\delta p(r,t) = \sum_{i=1}^{\infty} E_{ni}\left[J_n(\lambda_i r) - \frac{J_n(\lambda_i)}{Y_n(\lambda_i)}Y_n(\lambda_i r)\right]\cos(\theta)^n e^{-\frac{\lambda_i^2}{\sigma}t} \qquad [9]$$

The E_{ni} coefficients are determined by the initial conditions and are given in the appendix.

Integrating the pressure over the annulus area gives the corresponding force and moment.

$$\delta F_z(t) = \int_0^{2\pi}\int_{R_i}^{1} \delta p(r,t)\, r\, dr\, d\theta$$

$$\delta M_x(t) = \int_0^{2\pi}\int_{R_i}^{1} \delta p(r,t)\, r^2\cos(\theta)\, dr\, d\theta \qquad [10]$$

The full expressions for δF_z and δM_x are given here.

$$\partial F_z(t) = -2\pi\Delta z\sum_{i=1}^{\infty}\frac{E_{0i}}{\lambda_i}\left\{J_1(\lambda_i) - \frac{J_o(\lambda_i)}{Y_o(\lambda_i)}Y_1(\lambda_i) - R_i\left[J_1(\lambda_i R_i) - \frac{J_o(\lambda_i)}{Y_o(\lambda_i)}Y_1(\lambda_i R_i)\right]\right\}e^{-\frac{\lambda_i^2}{\sigma}t}$$

$$\delta M_x(t) = -\pi\Delta\gamma\sum_{i=1}^{\infty}\frac{E_{1i}}{\lambda_i}\left\{J_2(\lambda_i) - \frac{J_1(\lambda_i)}{Y_1(\lambda_i)}Y_2(\lambda_i) - R_i\left[J_2(\lambda_i R_i) - \frac{J_1(\lambda_i)}{Y_1(\lambda_i)}Y_2(\lambda_i R_i)\right]\right\}e^{-\frac{\lambda_i^2}{\sigma}t} \qquad [11]$$

The step responses are then calculated using the following relationships.

$$k_{fz}(t) = -\frac{\delta F_z(t)}{\Delta z} = 2\pi\sum_{i=1}^{\infty}\frac{E_{0i}}{\lambda_i}\left\{J_1(\lambda_i) - \frac{J_0(\lambda_i)}{Y_0(\lambda_i)}Y_1(\lambda_i) - R_i\left[J_1(\lambda_i R_i) - \frac{J_0(\lambda_i)}{Y_0(\lambda_i)}Y_1(\lambda_i R_i)\right]\right\}e^{-\frac{\lambda_i^2}{\sigma}t}$$

$$k_{my}(t) = -\frac{\delta M_x(t)}{\Delta\gamma} = \pi\sum_{i=1}^{\infty}\frac{E_{1i}}{\lambda_i}\left\{J_2(\lambda_i) - \frac{J_1(\lambda_i)}{Y_1(\lambda_i)}Y_2(\lambda_i) - R_i\left[J_2(\lambda_i R_i) - \frac{J_1(\lambda_i)}{Y_1(\lambda_i)}Y_2(\lambda_i R_i)\right]\right\}e^{-\frac{\lambda_i^2}{\sigma}t} \qquad [12]$$

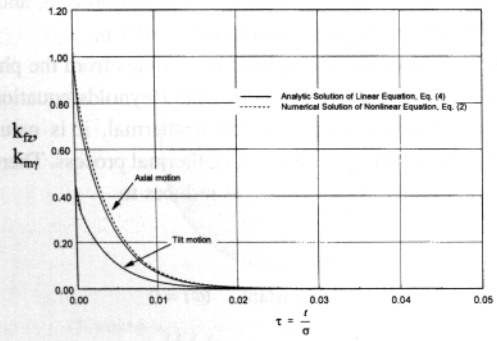

Fig. 3—Analytic and numerical solution for axial and tilt step responses (R_i=0.8).

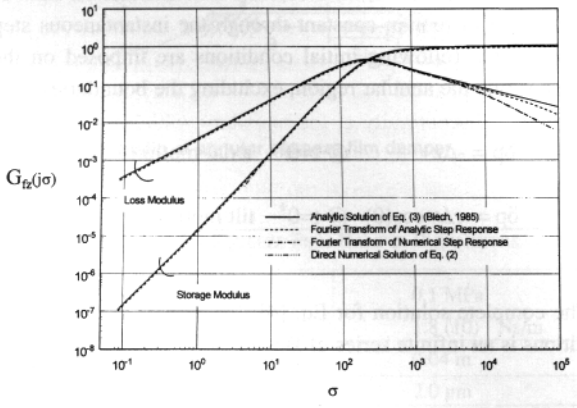

(a)

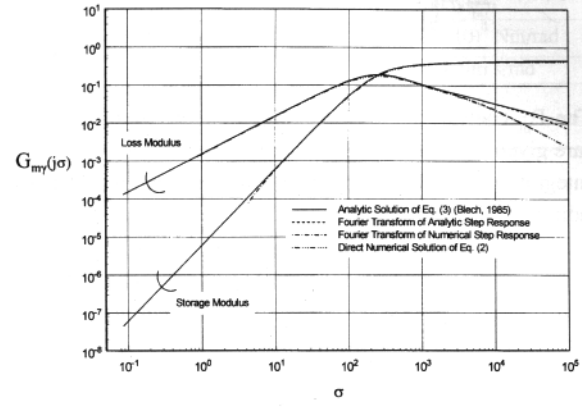

(b)

Fig. 4—(a) Frequency response for axial motion (R_i=0.8). (b) Frequency response for tilit motion (R_i=0.8).

For the parameters given in Table 1, the exact solutions for the step responses are shown in Figs. 2(a) and 2(b). The series in Eq. [12] was truncated to 15 terms because the remaining terms were two orders of magnitude or more smaller than the first term in the series. Along with the analytic solutions, the numerical solutions of the full nonlinear Reynolds equation are given in Fig. 3 for R_i=0.8. A detailed discussion of the method of calculating the step response numerically is given in Miller and Green (1997). Obviously, the analytic and numerical solutions are in very good agreement. This result is expected because the step jumps are very small and the perturbation assumptions are valid.

From the very nature of its definition in Eq. [12], it is clear that the step response represents the stiffness of the gas film. Motion of annulus A away from equilibrium leads to a pressure differential that acts as a restoring force. For this case, as seen in Figs. 2 and 3, the restoring force or moment decreases monotonically in time like the relaxation modulus of a viscoelastic material.

FREQUENCY RESPONSE

Just as the step response shows the gas film relaxation characteristics, the frequency response shows the dynamic properties of the gas film as a function of frequency. Specifically, the real part of the frequency response, $G'(j\sigma)$, corresponds to the storage modulus, and the imaginary part, $G''(j\sigma)$, corresponds to the loss modulus, such that $G(j\sigma)=G'(j\sigma) + j\, G''(j\sigma)$. The storage modulus correlates directly to the gas film stiffness, while the loss modulus is the damping multiplied by the frequency. The gas film frequency response is calculated here by four different methods. Results from these four methods are presented in Figs. 4(a) and 4(b). These curves show the typical nature of the gas film storage and loss moduli. The values at low frequencies represent a "rubbery" modulus. The curves go through a transition region and then level off to the values at high frequencies, which correspond to a "glassy" modulus.

Method 1

Analytic Solution for Frequency Response

The analytic solution for the gas film frequency response for annular compressible squeeze films is given by Blech (1985). The solution is restated here in Eqs. [13] and [14]. Recall again that n=0 corresponds to axial motion, and n=1 corresponds to tilt motion. See Abramowitz and Stegun (1972) for definitions of the Kelvin functions, ber_n, bei_n, ker_n, and kei_n. The coefficients, A_n, B_n, C_n, and D_n are given in the appendix.

$$\begin{aligned} G'_n(j\sigma) = \sqrt{\frac{4-3n}{2\sigma}}\Big\{ & A_n\Big[ber_{n+1}\sqrt{\sigma}+bei_{n+1}\sqrt{\sigma}-R_i^{n+1}\big(ber_{n+1}\sqrt{\sigma}R_i+bei_{n+1}\sqrt{\sigma}R_i\big)\Big] \\ & -B_n\Big[ber_{n+1}\sqrt{\sigma}-bei_{n+1}\sqrt{\sigma}-R_i^{n+1}\big(ber_{n+1}\sqrt{\sigma}R_i-bei_{n+1}\sqrt{\sigma}R_i\big)\Big] \\ & +C_n\Big[\mathrm{ker}_{n+1}\sqrt{\sigma}+kei_{n+1}\sqrt{\sigma}-R_i^{n+1}\big(\mathrm{ker}_{n+1}\sqrt{\sigma}R_i+kei_{n+1}\sqrt{\sigma}R_i\big)\Big] \\ & -D_n\Big[\mathrm{ker}_{n+1}\sqrt{\sigma}-kei_{n+1}\sqrt{\sigma}-R_i^{n+1}\big(\mathrm{ker}_{n+1}\sqrt{\sigma}R_i-kei_{n+1}\sqrt{\sigma}R_i\big)\Big]\Big\}+\frac{1-R_i^{2n+2}}{3n+1} \end{aligned} \quad [13]$$

$$\begin{aligned} G''_n(j\sigma) = -\sqrt{\frac{4-3n}{2\sigma}}\Big\{ & A_n\Big[ber_{n+1}\sqrt{\sigma}-bei_{n+1}\sqrt{\sigma}-R_i^{n+1}\big(ber_{n+1}\sqrt{\sigma}R_i-bei_{n+1}\sqrt{\sigma}R_i\big)\Big] \\ & +B_n\Big[ber_{n+1}\sqrt{\sigma}+bei_{n+1}\sqrt{\sigma}-R_i^{n+1}\big(ber_{n+1}\sqrt{\sigma}R_i+bei_{n+1}\sqrt{\sigma}R_i\big)\Big] \\ & +C_n\Big[\mathrm{ker}_{n+1}\sqrt{\sigma}-kei_{n+1}\sqrt{\sigma}-R_i^{n+1}\big(\mathrm{ker}_{n+1}\sqrt{\sigma}R_i-kei_{n+1}\sqrt{\sigma}R_i\big)\Big] \\ & +D_n\Big[\mathrm{ker}_{n+1}\sqrt{\sigma}+kei_{n+1}\sqrt{\sigma}-R_i^{n+1}\big(\mathrm{ker}_{n+1}\sqrt{\sigma}R_i+kei_{n+1}\sqrt{\sigma}R_i\big)\Big]\Big\} \end{aligned} \quad [14]$$

The analytic solution shown in Fig. 4 compares well with the other three methods, except for a small, consistent offset in the storage modulus. An explanation for this offset is discussed later. One discrepancy between this method and the other three methods, however, does appear in the loss modulus. The slope in the analytic solution for the loss modulus is more gradual at very high frequencies compared to the other three methods. Because the dif-

ference occurs at such high frequency and the magnitude of the loss modulus at these frequencies is relatively low, this discrepancy is negligible.

Method 2

Numerical Solution for Frequency Response

The gas film frequency response can also be found by a direct numerical method. In this approach, Annulus A is given sinusoidal oscillations of the form

$$\delta h = \Delta h \sin(t) \qquad [15]$$

for the axial motion and

$$\delta h = r\Delta\gamma \cos(\theta) \sin(t) \qquad [16]$$

for the tilt motion. The translational and tilt amplitudes, respectively, are chosen to be Δh=0.05 and $\Delta\gamma$=0.01, which are within the range of small perturbation. Equations [15] and [16] are then substituted into Eq. [2], and the solution is computed numerically using the finite difference method and a Runge-Kutta time integration technique. At each time step, the displacement of Annulus A is stored, and the total force and moment on Annulus A is also computed and stored. The time solution is computed for at least four cycles to ensure that any transient dynamic motion has dissipated. Next, the spectra of the displacement, force, and moment, $\delta H(j\sigma)$, $\delta F_z(j\sigma)$ and $\delta M_x(j\sigma)$ respectively, are calculated digitally by a fast Fourier transform (FFT). Then, the gas film frequency responses are found at each frequency using the relations below.

$$G_{fz}(j\sigma) = \frac{\delta F_z(j\sigma)}{\delta H(j\sigma)}$$
$$G_{m\gamma}(j\sigma) = \frac{\delta M_x(j\sigma)}{\delta H(j\sigma)} \qquad [17]$$

As seen in Fig. 4, the results from this method are in excellent agreement with the results from the other methods. This method, however, is computationally intensive and time consuming.

Method 3

Fourier Transform of the Analytic Step Response

According to the step jump method (Elrod et al., 1967), the gas film properties can also be characterized in the time domain by the step response. The frequency response can be computed directly from the step response using the following cosine and sine transformations (Miller and Green, 1998).

$$G'(j\sigma) = \int_0^\infty \dot{k}(t)\cos(t)\, dt$$
$$G''(j\sigma) = -\int_0^\infty \dot{k}(t)\sin(t)\, dt \qquad [18]$$

Substituting the analytic solution for the step response, Eq. [12], into Eq. [18] yields,

$$G_{fz}(j\sigma) = 2\pi\sum_{i=1}^{\infty}\frac{E_{0i}}{\lambda_i}\left\{J_1(\lambda_i) - \frac{J_0(\lambda_i)}{Y_0(\lambda_i)}Y_1(\lambda_i) - R_i\left[J_1(\lambda_i R_i) - \frac{J_0(\lambda_i)}{Y_0(\lambda_i)}Y_1(\lambda_i R_i)\right]\right\}\frac{j\sigma}{\lambda_i^2 + j\sigma}$$
$$G_{m\gamma}(j\sigma) = \pi\sum_{i=1}^{\infty}\frac{E_{1i}}{\lambda_i}\left\{J_2(\lambda_i) - \frac{J_1(\lambda_i)}{Y_1(\lambda_i)}Y_2(\lambda_i) - R_i\left[J_2(\lambda_i R_i) - \frac{J_1(\lambda_i)}{Y_1(\lambda_i)}Y_2(\lambda_i R_i)\right]\right\}\frac{j\sigma}{\lambda_i^2 + j\sigma} \qquad [19]$$

Although they are in closed form, the equations in Eq. [19] are not equivalent to the analytic solutions for the frequency response given in Eqs. [13] and [14], even if the series were allowed to approach infinity. The difference results from the physical impossibility imposed by the assumption in the step response at t=0, which requires the pressure everywhere inside the annular region to instantaneously jump to a quantity proportional to the step jump amplitude, except at the boundaries. This assumption thus results in a pressure discontinuity at the boundary, which is physically impossible. This assumption at low times near t=0 manifests through the Fourier transform as an offset in the frequency response approximation at large frequency.

This offset is evident in the plot of the gas film storage modulus for axial motion in Fig. 4(a). The asymptotic value for the axial motion stiffness given by the analytic solution is approximately 1.12. For the approximation by Fourier transformation of the analytic step response, the asymptotic stiffness value is approximately 1.00, representing an 11 percent offset. This offset is not evident in the axial motion loss modulus, however, because the high frequency damping approaches zero. Notice also that the offset is negligible for the tilt motion storage modulus. In this case, the symmetry condition about the x axis negates any discrepancy in the pressure field at the boundary that occurs in the time immediately following the step jump. Overall, the other properties of the frequency response, such as the shape of the curves and the transition region between the rubbery and glassy moduli, are predicted well.

Method 4

Fourier Transform of the Numerical Step Response

As stated earlier, k(t) can also be computed by numerical solution of Eq. [2] (Miller and Green, 1997). In such a case, an approximation for the frequency response can be found by numerical evaluation of the integrals in Eq. [18]. Results from this method are in very good agreement with the results from the previous methods (see Figs. 4(a) and 4(b)).

Numerical Solution Considerations

The efficiency of numerical algorithms is of growing concern lately. Naturally, the fastest running code possible is preferred, so long as solution accuracy is not sacrificed. The numerical solutions for the step responses were calculated with a finite difference algorithm using 13 nodes to span the radius and 60 nodes around the circumference, totaling 780 nodes. With this number of nodes, it took approximately one minute and six seconds to calculate each step response on an IBM RISC 6000, Model R50 computer.

TABLE 2—PRONY SERIES COEFFICIENTS FOR THE CONSTITUTIVE MODELS (K(∞)=0)

	Method	Analytic Frequency Response		Numerical Frequency Response		Analytic Step Response		Numerical Step Response	
	n	Q_n	α_n	Q_n	α_n	Q_n	α_n	Q_n	α_n
Axial	1	0.9444	255.07	0.89096	248.24	0.8511	253.45	0.9130	246.82
	2	0.1601	5842.87	0.1437	2640.93	0.1422	4986.10	0.1216	2599.20
Tilt	1	0.3850	257.30	0.3628	250.86	0.3827	255.38	0.3711	248.23
	2	0.0676	5782.86	0.0601	2576.59	0.0658	4948.08	0.0520	2532.25

Generating the frequency response numerically required much more computing effort, for the above procedure must be repeated for each frequency point. Therefore, the computing time is directly proportional to the number of data points needed to adequately portray the character of the curve. Data points for twenty different frequencies are shown in Figs. 4(a) and 4(b). Generating this data required 18 hours and 45 minutes of computing time on the same computer, which is roughly three orders of magnitude longer than needed for the step response. Obviously, it is important to take advantage of the most efficient technique to decrease the amount of computing time. The step jump method gives this advantage by offering a considerable computational savings with little sacrifice in accuracy.

APPLICATION OF THE GAS FILM CORRESPONDENCE PRINCIPLE

After the step response or frequency response is found, the next step is to store this information in analytic form by approximating the curves (either in the time or frequency domains) with an analytic function. This process creates a constitutive model for the gas film. The constitutive model represents a kernel of solution of the Reynolds equation. Once this kernel is found, the equations of motion can be solved analytically and closed form solutions can be rendered, when possible, i.e., when the inverse Laplace transform can be found analytically. The gas film constitutive model is incorporated into the equations of motion using the gas film correspondence principle (Miller and Green, 1998).

Both Szumski (1993) and Miller and Green (1998) have had success using a Prony series (a series of decaying exponential functions) for the constitutive model. This result should be expected because the analytic solution for the step response from the linearized form of the Reynolds equation is a series of decaying exponential functions in Eq. [12]. Since the gas film correspondence principle formulates the solution for the equations of motion in the Laplace domain, the Prony series form for the constitutive model is useful because it has both time and Laplace domain representations. The Prony series approximation of the step response is given below.

$$k(t) = k(\infty) + \sum_{n=1}^{N} Q_n e^{-\alpha_n t} \qquad [20]$$

where α_n are the decay parameters and Q_n are constant coefficients. The Laplace transform of Eq. [20] is given below.

$$sK(s) = k(\infty) + \sum_{n=1}^{N} Q_n \frac{s}{s+\alpha_n} \qquad [21]$$

where K(s) is the Laplace transform of k(t). Replacing s with jσ gives the frequency response.

$$G(j\sigma) = j\sigma K(j\sigma) = k(\infty) + \sum_{n=1}^{N} Q_n \frac{j\sigma}{j\sigma+\alpha_n} \qquad [22]$$

The value for k(∞) is the asymptotic value of the step response, which is identically zero for this application. Table 2 gives the values for the four gas film constitutive models, which were derived from the analytic and numerical solutions for both the frequency response and step response. Although the analytic solution for the step response is already in an acceptable form, a curve fit was still performed to greatly reduce the number of terms from 15 down to two. These values for Q_n, and α_n were determined using a multivariable function minimizing process with a Nelder-Mead simplex algorithm using MATLAB software from The MathWorks, Inc. These constitutive models become an exact fit of the curves if the number of terms in the approximation, N, is allowed to approach infinity. However, a very large number of terms is impractical for computing purposes. The number of terms can be chosen either by a trial and error method or by applying a criterion to measure the quality of fit. In this work, a one term Prony series gives sufficiently accurate fits. This number was chosen by a trial and error procedure.

The first step in using the gas film correspondence principle is to formulate the equations of motion in the time domain. The equations of motion are given below for the geometry in Fig. 1,

$$\begin{aligned} m\ddot{z} &= \delta F_z - k_{sz} z - d_{sz}\dot{z} \\ I\ddot{\gamma} &= \delta M_x - k_{s\gamma}\gamma - d_{s\gamma}\dot{\gamma} \end{aligned} \qquad [23]$$

where δF_z is the net force in the z direction from the gas film, and δM_x is the net moment from the gas film about the x axis. At first, the net gas film force and moment are modeled as pseudo linear springs with spring moduli, k_{gz} and $k_{g\gamma}$

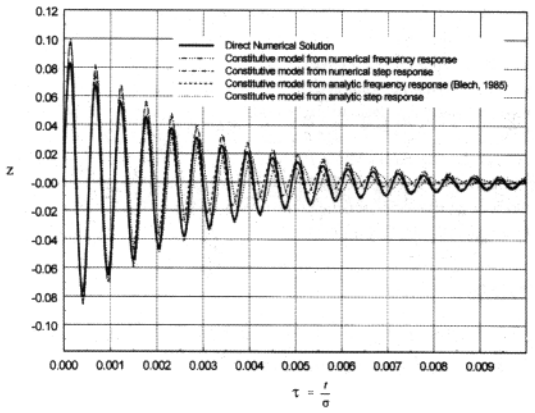

Fig. 5—Axial response of Annulus A to an initial velocity of $2(10)^{-3}$ m/s (R_i=0.8).

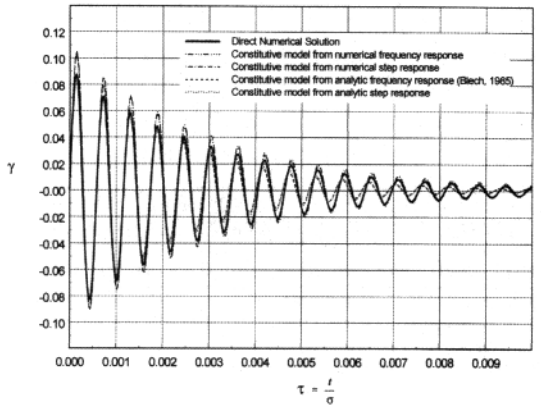

Fig. 6—Tilt response of Annulus A to an initial angular velocity about the x-axis of $5(10)^{-2}$ rad/s (R_i=0.8).

$$m\ddot{z} = -k_{gz}z - k_{sz}z - d_{sz}\dot{z}$$
$$I\ddot{\gamma} = -k_{g\gamma}\gamma - k_{s\gamma}\gamma - d_{s\gamma}\dot{\gamma} \qquad [24]$$

After transforming the equations into the Laplace domain, the dynamic properties of the gas film are incorporated into the problem by employing the gas film correspondence principle, i.e., by replacing the pseudo stiffnesses, k_{gz} and $k_{g\gamma}$, with $sK_{fz}(s)$ and $sK_{m\gamma}(s)$, respectively, giving

$$m\left[s^2Z(s) - sz(0) - \dot{z}(0)\right] = -sK_{fz}(s)Z(s) - k_{sz}Z(s) - d_{sz}\left[sZ(s) - z(0)\right]$$
$$I\left[s^2\Gamma(s) - s\gamma(0) - \dot{\gamma}(0)\right] = -sK_{m\gamma}(s)\Gamma(s) - k_{s\gamma}\Gamma(s) - d_{s\gamma}\left[s\Gamma(s) - \gamma(0)\right] \qquad [25]$$

The characteristic equations are easily extracted,

TABLE 3—NONDIMENSIONAL NATURAL OSCILLATION FREQUENCIES OF ANNULUS A (R_i=0.8)

METHOD	AXIAL	TILT
Direct Numerical Simulation	11505	10815
Correspondence principle with the constitutive model from the analytic frequency response, Eqs. [13] and [14] (Blech, 1985)	11635	10939
Correspondence principle with the constitutive model from the analytic step response, Eq. [12]	11283	10939
Correspondence principle with the constitutive model from the numerical frequency response	11493	10820
Correspondence principle with the consitutive model from the numerical step response	11499	10825

$$ms^2 + sK_{fz}(s) + k_{sz} + sd_{sz} = 0$$
$$Is^2 + sK_{m\gamma}(s) + k_{s\gamma} + sd_{s\gamma} = 0 \qquad [26]$$

The roots of these equations are the system eigenvalues. An explicit expression for the motion of Annulus A can be written as follows.

$$Z(s) = \frac{m\left[z(0)s + \dot{z}(0)\right] + d_{sz}z(0)}{ms^2 + sK_{fz}(s) + k_{sz} + d_{sz}s} \quad \Gamma(s) = \frac{I\left[\gamma(0)s + \dot{\gamma}(0) + d_{s\gamma}\gamma(0)\right]}{Is^2 + sK_{m\gamma}(s) + k_{s\gamma} + d_{s\gamma}s} \qquad [27]$$

The time histories of displacement are now available by obtaining the inverse Laplace transform of Z(s) and Γ(s) either analytically or numerically.

As an example, the plots shown in Figs. 5 and 6 show the time response of Annulus A to an initial axial velocity of $2(10)^{-3}$ m/s and an initial tilt velocity of $5(10)^{-2}$ rad/s. Note that the axial force in response to tilt motion is negligible and the moment about the x axis in response to axial motion is identically zero. Therefore, the axial and tilt degrees of freedom are completely decoupled in Eq. [23]. These figures plot the results from the gas film correspondence principle using the four constitutive models and the results predicted by a direct numerical solution of Eq. [2] coupled with the equation of motion. Both the axial and the tilt motions appear to be underdamped sinusoidal vibrations. The natural frequencies of oscillation from all the methods are summarized in Table 3. The frequencies predicted by the correspondence principle with the constitutive models from both the numerical frequency response and numerical step response are very close to the oscillation frequency from the direct numerical simulation. The oscillation frequencies predicted by the correspondence principle with the other two methods are also within two percent of the frequency from the direct numerical method. The quality of the prediction of damping is not as easy to quantify as the oscillation frequency. However, a visual comparison of the decay envelope provides some way to

measure the quality of the damping prediction. The decay rates predicted by the correspondence principle with all four constitutive models are close to the decay rate from the direct numerical simulation.

All these curves are in good agreement with the motion predicted by the direct numerical simulation, which suggests that each constitutive model is a good representation of the gas film characteristics. The accuracy achieved by the correspondence principle is not surprising since the curve fits for the constitutive models are close near the natural frequencies of oscillation. If the annulus oscillated at a frequency where the constitutive model and the actual frequency response did not match up well, then the predicted values would be less accurate. However, in special cases when it is known in advance that the system will oscillate at frequencies in a certain bandwidth, it is possible to adjust the curve fitting algorithm to emphasize the frequency band of interest and minimize the relative error.

CONCLUSION

The gas film is a key element in the overall dynamics of gas lubricated triboelements. Knowing either the gas film frequency response or step response is important because they are clear and compact representations of the dynamic properties of the gas film. The step jump method is proven to give a good approximation for the frequency response for annular shaped gas film squeeze dampers. Results from the step jump method compare well to a direct analytic solution for the frequency response as well as a direct numerical solution. The step jump method offers a significant time savings compared to calculating the frequency response directly by a numerical procedure.

Once the step response or the frequency response is computed, it is possible to develop a constitutive model for the gas film. The constitutive model is formed by approximating the step response or the frequency response with an analytic function. In this case, a Prony series is chosen as the constitutive model. The stiffness and damping of the gas film are then incorporated into the overall system model using the gas film correspondence principle. Closed form solutions are found for the motion of Annulus A, and they compare well to solutions from a conventional, direct numerical method.

ACKNOWLEDGMENT

This work was supported in part by an NSF Graduate Research Traineeship through Grant No. EEC-9256289. This support is gratefully acknowledged.

REFERENCES

(1) Abramowitz, M., and Stegun, I. A., ed., *Handbook of Mathematical Functions*, National Bureau of Standards, Applied Math Series, **55**, (1972).

(2) Blech, J. J., "Annular Compressible Squeeze Films," *ASME Jour. of Trib.*, **107**, 4, pp 544-547, (1985).

(3) Green, I. and Etsion, I., "Stability Threshold and Steady-State Response of Noncontacting Coned-Face Seals," *ASLE Trans.*, **28**, pp 449-460, (1985).

(4) Elrod, H. G., Jr., McCabe, J. T. and Chu, T. Y., "Determination of Gas-Bearing Stability by Response to a Step-Jump," *ASME Jour. of Lubr. Tech.*, **89**, pp 493-498, (1967).

(5) Etsion, I., "The Accuracy of the Narrow Seal Approximation in Analyzing Radial Face Seals," *ASLE Trans.*, **23**, 2, pp 208-216, (1980).

(6) Miller, B. and Green, I., "On the Stability of Gas Lubricated Triboelements Using the Step Jump Method," *ASME Jour. of Trib.*, **119**, 1, pp 193-199, (1997).

(7) Miller, B. and Green, I., "Constitutive Equations and the Correspondence Principle for the Dynamics of Gas Lubricated Triboelements," *ASME Jour. of Trib.*, **120**, 2, pp 345-352, (1998).

(8) Ono, K., "Dynamic Characteristics of Air-Lubricated Slider Bearing for Noncontact Magnetic Recording," *ASME Jour. of Lubr. Tech.*, **97**, pp 250-260, (1975).

(9) Powers, D. L., *Boundary Value Problems*, 3rd Ed., Harcourt Brace, (1987).

(10) Szumski, R. G., "A Finite Element Formulation for the Time Domain Vibration Analysis of an Elastic-Viscoelastic Structure," Ph.D. Thesis, Georgia Institute of Technology, Atlanta, GA, (1993).

APPENDIX

The coefficients, E_{ni}, of the infinite series solution for the pressure given in Eq. [9] is given below.

$$E_{0i} = \frac{2\Delta z}{\lambda_i} \frac{\left\{ J_1(\lambda_i) + \frac{J_0(\lambda_i)}{Y_0(\lambda_i)} Y_1(\lambda_i) - R_i \left[J_1(\lambda_i R_i) + \frac{J_0(\lambda_i)}{Y_0(\lambda_i)} Y_1(\lambda_i R_i) \right] \right\}}{\left\{ J_1(\lambda_i) + \frac{J_0(\lambda_i)}{Y_0(\lambda_i)} Y_1(\lambda_i) \right\}^2 - \left\{ R_i \left[J_1(\lambda_i R_i) + \frac{J_0(\lambda_i)}{Y_0(\lambda_i)} Y_1(\lambda_i R_i) \right] \right\}^2} \quad [28]$$

$$E_{1i} = \frac{2\Delta \gamma}{\lambda_i} \frac{\left\{ J_2(\lambda_i) + \frac{J_1(\lambda_i)}{Y_1(\lambda_i)} Y_2(\lambda_i) - R_i \left[J_2(\lambda_i R_i) + \frac{J_1(\lambda_i)}{Y_1(\lambda_i)} Y_2(\lambda_i R_i) \right] \right\}}{\left\{ J_0(\lambda_i) + \frac{J_1(\lambda_i)}{Y_1(\lambda_i)} Y_0(\lambda_i) \right\}^2 - \left\{ R_i \left[J_0(\lambda_i R_i) + \frac{J_1(\lambda_i)}{Y_1(\lambda_i)} Y_0(\lambda_i R_i) \right] \right\}^2} \quad [29]$$

The coefficients A_n, B_n, C_n, and D_n of Eqs. [13] and [14] are given here. They are also given in the appendix of Blech (1985), and the D_n coefficient, which is printed incorrectly there, is corrected here.

$$\begin{aligned} A_n = \frac{1}{d_n} \{ & bei_n\sqrt{\sigma}\left(\ker_n^2\sqrt{\sigma R_i}\right) + \ker_n\sqrt{\sigma}\left(kei_n\sqrt{\sigma R_i} ber_n\sqrt{\sigma R_i} - bei_n\sqrt{\sigma R_i}\ker_n\sqrt{\sigma R_i}\right) \\ & - kei_n\sqrt{\sigma}\left(bei_n\sqrt{\sigma R_i} kei_n\sqrt{\sigma R_i} ber_n\sqrt{\sigma R_i}\right) + R_i^n\left[bei_n\sqrt{\sigma R_i}\left(\ker_n^2\sqrt{\sigma} + kei_n^2\sqrt{\sigma}\right) \right. \\ & \left. + \ker_n\sqrt{\sigma R_i}\left(kei_n\sqrt{\sigma} ber_n\sqrt{\sigma} - bei_n\sqrt{\sigma}\ker_n\sqrt{\sigma}\right) - kei_n\sqrt{\sigma R_i}\left(bei_n\sqrt{\sigma} kei_n\sqrt{\sigma} + \ker_n\sqrt{\sigma} ber_n\sqrt{\sigma}\right) \right] \} \end{aligned} \quad [30]$$

$$\begin{aligned} B_n = \frac{1}{d_n} \{ & ber_n\sqrt{\sigma}\left(\ker_n^2\sqrt{\sigma R_i} + kei_n^2\sqrt{\sigma R_i}\right) + \ker_n\sqrt{\sigma}\left(ber_n\sqrt{\sigma R_i}\ker_n\sqrt{\sigma R_i} + kei_n\sqrt{\sigma R_i} bei_n\sqrt{\sigma R_i}\right) \\ & - kei_n\sqrt{\sigma}\left(\ker_n\sqrt{\sigma R_i} bei_n\sqrt{\sigma R_i} - ber_n\sqrt{\sigma R_i} kei_n\sqrt{\sigma R_i}\right) + R_i^n\left[-ber_n\sqrt{\sigma R_i}\left(\ker_n^2\sqrt{\sigma} + kei_n^2\sqrt{\sigma}\right) \right. \\ & \left. + \ker_n\sqrt{\sigma R_i}\left(ber_n\sqrt{\sigma}\ker_n\sqrt{\sigma} + kei_n\sqrt{\sigma} bei_n\sqrt{\sigma}\right) - kei_n\sqrt{\sigma R_i}\left(\ker_n\sqrt{\sigma} bei_n\sqrt{\sigma} - ber_n\sqrt{\sigma} kei_n\sqrt{\sigma}\right) \right] \} \end{aligned} \quad [31]$$

$$\begin{aligned} C_n = \frac{1}{d_n} \{ & kei_n\sqrt{\sigma}\left(ber_n^2\sqrt{\sigma R_i} + bei_n^2\sqrt{\sigma R_i}\right) + ber_n\sqrt{\sigma}\left(bei_n\sqrt{\sigma R_i}\ker_n\sqrt{\sigma R_i} - kei_n\sqrt{\sigma R_i} ber_n\sqrt{\sigma R_i}\right) \\ & - bei_n\sqrt{\sigma}\left(ber_n\sqrt{\sigma R_i}\ker_n\sqrt{\sigma R_i} + kei_n\sqrt{\sigma R_i} bei_n\sqrt{\sigma R_i}\right) + R_i^n\left[kei_n\sqrt{\sigma R_i}\left(ber_n^2\sqrt{\sigma} + bei_n^2\sqrt{\sigma}\right) \right. \\ & \left. + ber_n\sqrt{\sigma R_i}\left(bei_n\sqrt{\sigma}\ker_n\sqrt{\sigma} - kei_n\sqrt{\sigma} ber_n\sqrt{\sigma}\right) - bei_n\sqrt{\sigma R_i}\left(ber_n\sqrt{\sigma}\ker_n\sqrt{\sigma} + kei_n\sqrt{\sigma} bei_n\sqrt{\sigma}\right) \right] \} \end{aligned} \quad [32]$$

$$\begin{aligned} D_n = \frac{1}{d_n} \{ & -\ker_n\sqrt{\sigma}\left(ber_n^2\sqrt{\sigma R_i} + bei_n^2\sqrt{\sigma R_i}\right) + ber_n\sqrt{\sigma}\left(bei_n\sqrt{\sigma R_i} kei_n\sqrt{\sigma R_i} + \ker_n\sqrt{\sigma R_i} ber_n\sqrt{\sigma R_i}\right) \\ & + bei_n\sqrt{\sigma}\left(\ker_n\sqrt{\sigma R_i} bei_n\sqrt{\sigma R_i} - ber_n\sqrt{\sigma R_i} kei_n\sqrt{\sigma R_i}\right) + R_i^n\left[-\ker_n\sqrt{\sigma R_i}\left(ber_n^2\sqrt{\sigma} + bei_n^2\sqrt{\sigma}\right) \right. \\ & \left. + ber_n\sqrt{\sigma R_i}\left(bei_n\sqrt{\sigma}\ker_n\sqrt{\sigma} + \ker_n\sqrt{\sigma} ber_n\sqrt{\sigma}\right) + bei_n\sqrt{\sigma R_i}\left(\ker_n\sqrt{\sigma} bei_n\sqrt{\sigma} - ber_n\sqrt{\sigma} kei_n\sqrt{\sigma}\right) \right] \} \end{aligned} \quad [33]$$

where

$$\begin{aligned} d_n = & \left(ber_n\sqrt{\sigma R_i} - \ker_n\sqrt{\sigma} ber_n\sqrt{\sigma R_i}\right)^2 + \left(bei_n\sqrt{\sigma}\ker_n\sqrt{\sigma R_i} - \ker_n\sqrt{\sigma R_i}\right)^2 \\ & + \left(ber_n\sqrt{\sigma} kei_n\sqrt{\sigma R_i} - kei_n\sqrt{\sigma R_i} ber_n\sqrt{\sigma R_i}\right)^2 + \left(bei_n\sqrt{\sigma} kei_n\sqrt{\sigma R_i} - kei_n\sqrt{\sigma} bei_n\sqrt{\sigma R_i}\right)^2 \\ & + 2\left(\ker_n\sqrt{\sigma} kei_n\sqrt{\sigma R_i} - kei_n\sqrt{\sigma}\ker_n\sqrt{\sigma R_i}\right)\left(bei_n\sqrt{\sigma} ber_n\sqrt{\sigma R_i} - ber_n\sqrt{\sigma} bei_n\sqrt{\sigma R_i}\right) \end{aligned} \quad [34]$$

See Abramowitz and Stegun (1972) for definitions of the Kelvin functions, ber_n, bei_n, ker_n, and kei_n.